

OPC resist model separability validation after SMO source change

Werner Gillijns^{*a}, Jeroen Van de Kerkhove^a, Darko Trivkovic^a, Peter De Bisschop^a,

David Rio^b, Stephen Hsu^b, Mu Feng^b, Qiang Zhang^b, Hua-yu Liu^b

^aimec vzw, Kapeldreef 75, B-3001 Leuven, Belgium

^bASML Brion, 4211 Burton Dr., Santa Clara, CA, 95054, USA

ABSTRACT

Computational lithography has become indispensable when developing lithography solutions for advanced technology nodes. One of the essential instruments for optimizing full-chip process windows (PW) is source mask optimization (SMO). To avoid model calibration for each new optimized source, separable resist models need to be created such that a reliable model can be obtained simply by replacing the source in the existing OPC model.

In this paper we start from a fully calibrated resist model and optimize a new source for which we want to create a reliable OPC model. Relying on the separability of the model, the initial illumination source is replaced by the new one while not changing any resist model parameters. In order to reach the accuracy needed for OPC, the best focus and best dose still need to be accurately determined. We will investigate two models that have the same new SMO source and original resist model. For one model the best focus and dose are determined by the simulated Bossung plot of one anchor feature. The second model's best focus and exposure are determined by a small set of FEM experimental data. The quality of these two models is then evaluated by comparing them to a reference model, which is fully calibrated using a complete dataset for the new source.

We show that the calibrated FEM OPC model can be extrapolated by simply changing the source. A limited amount of experimental FEM data is required to accurately determine the best focus and exposure for the new source. Best focus and exposure based on the anchor pattern simulation has a higher degree of uncertainty compared to a small set of experimental data.

Keywords: Tachyon SMO, OPC model calibration, computational lithography, FEM model, LMC, experimental model-quality verification, separability

1. INTRODUCTION

Separable OPC models attempt to model each physical and chemical step in the lithography process in discrete modules. When the resist, optical and mask module each stand distinctly, changing one part of the physical process should only affect the corresponding module of the model. Tachyon FEM+ models have been shown to be separable to a high degree for parametric sources^{1,2}. It was shown that an OPC model, initially calibrated for one illumination condition, still obtained good predicting power after the illumination condition of the parametric source was altered.

Since the introduction of Tachyon SMO, which can optimize a source for specific applications, the need for separable models has become even more apparent. A full-chip optimization exercise starts with optimizing a source using SMO. Typically the SMO is run with an existing calibrated resist model as input. The output of SMO is a new optimized source which could invalidate the initial model if no separability is achieved. So before moving to OPC on the full chip, a re-calibration would have to be performed. To avoid this lengthy calibration after each SMO-run it is important to create separable resist models.

In this paper we want to investigate the separability of Tachyon FEM+ models, taking the case of a 20 nm node LELE Metal1 application using Negative Tone Development (NTD)³. We start from an existing resist model (M1) which is calibrated for a given FlexRay source (S1). The goal is then to create a reliable resist model for the same process but using a different FlexRay source (S2). As can be seen in figure 1(a), S2 is significantly different from S1. For this SMO optimization, S2 has a best-dose which is 32% lower than S1. We created three different models for our investigation (see Fig. 1):

* werner.gillijns@imec.be; phone +32 16 281627

- (i) A model which is created by replacing the source and keeping the original resist parameters (R1) from M1, followed by anchoring the best dose and best focus based on the simulated Bossung of the anchor (M2S).
- (ii) The second model keeps the same resist model parameters as well but in order to determine the best focus and best dose more reliably, a small experimental dataset is used instead of relying completely on the simulated anchor feature (M2E).
- (iii) A model which is completely re-calibrated, according to our best practice (M2). Since this is the best model we can obtain for this source, we regard this model as the target for models M2S and M2E (see figure 1).

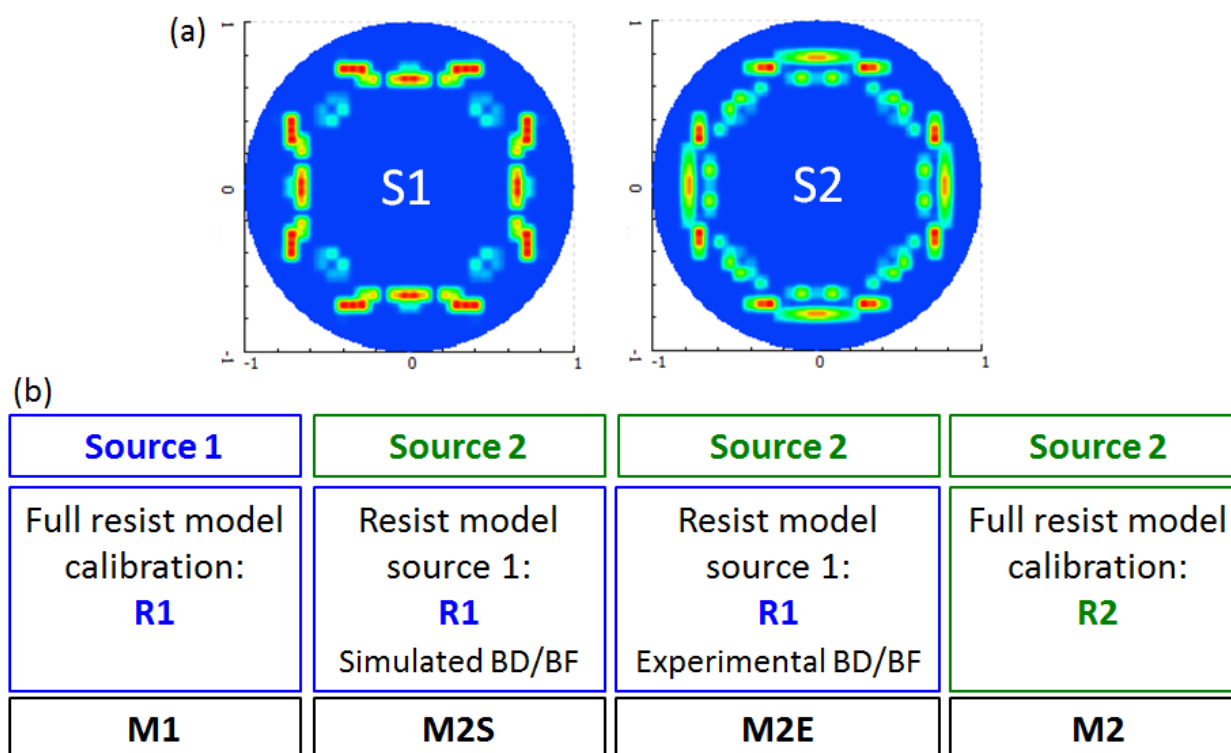


Figure 1: (a) FlexRay illuminator profile of source 1 and source 2. (b) Schematic overview of all resist models under investigation.

In the following section we will describe our procedure to obtain the experimental data on 1D and 2D gauges for the full model calibration of model M2. Section 3 will go into detail about the calibration of the models under investigation. These models will be evaluated in section 4 in three ways. Firstly, we evaluate the RMS of the model error on the calibration and verification features. Secondly, we investigate the error of the calculated contour of the M2S and M2E models with respect to the reference model M2 on our 20nm node logic Metal1 layer. And thirdly, we will quantify the penalty in process window for this metal layer by using model M2E and M2S during OPC instead of M2. We conclude in section 5.

2. GAUGE MEASUREMENTS & REFERENCE-MODEL CALIBRATION

We have used a 20 nm node LELE Metal1 Logic application as the test vehicle for the study of this paper. All wafer exposures were done on an SOG/SOC type LELE compatible stack that was also adapted to allow for a 15 nm litho bias and subsequent 15 nm shrink of the CDs in the etch process. We used negative-tone development (NTD) from FujiFilm (FAiRS-9521M190) and an NTD-dedicated resist, and hence a bright-field mask to print trenches in resist.

The calibration of the reference models (M1 and M2) was done according to a procedure that we standardly use at imec. This means that the selection of the gauges used for the calibration and verification step of the models is based on the basic design rules of the application, i.e. considering the pitches and tip-to-tip and tip-to-line gaps that are expected in the application. For example, the minimum Metal1 pitches in the logic test-clips we used in this study were 90 and 64 nm (vertical and horizontal orientation respectively) before split. In each of the split layers, the minimum allowed pitch was 90 nm. From this type of design information, we then selected sets of 1D (e.g. L/S structures, with and without assist features, as well as trench doublets and triplets) and 2D (e.g. end-of-line but also more complicated) structures for model-calibration measurements. Over 300 different structures were used for model calibration, and about the same number for model verification. Through-focus and –dose measurements were done for a subset of these, covering a defocus range of $\pm 50\text{nm}$ and a dose-offset range of $\pm 6\%$. All the models in this paper were generated using Brion's mask-3D (M3D) option³.

For evaluation of the model quality, several metrics can be used, applying them preferentially on verification structures that are independent from the structures used for model calibration. The starting point is then of course the individual residual model error values, ΔCD , i.e. the difference between the measured and predicted CDs for all structures, dose- and focus-conditions. These are then traditionally combined into a single RMS value, but figure 2 illustrates a few other possibilities. Figure 2(a) and (b), for example, consider only ΔCD values from nominal focus- and dose-conditions, plotting them in a histogram or versus some structure-specific design parameter. Figure 2(c) summarizes the quality of the predicted Process Window (PW) data, by calculating a separate RMS value for every individual structure for which PW data was measured.

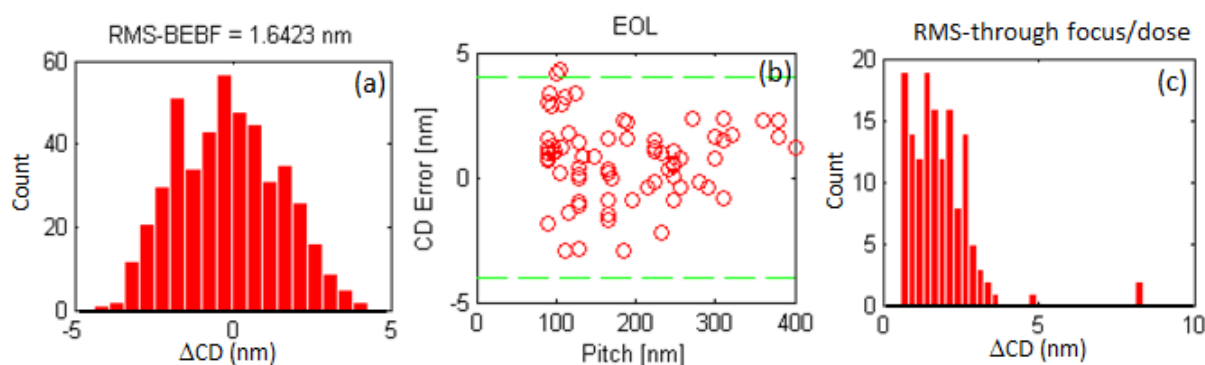


Figure 2: Illustration of some of the metrics we use to evaluate the quality of our OPC models: example of model M1, verification structures only. (a) Histogram of all the residual model error ΔCD data, from measurements in nominal focus and dose conditions. (b) Nominal-condition ΔCD data, now for the tip-to-tip and tip-to-line structures only, plotted vs. the L/S pitch, to demonstrate the absence of any residual trends. (c) Histogram of RMS values calculated individually for each structure for which there are through-focus and –dose measurements.

3. MODEL TUNING

The Tachyon FEM+ model platform represents the real lithography process in a pipeline structure with a set of separable modules, such as mask, optical, resist and etch. If a FEM+ model has been qualified to have sufficient full chip prediction power within the process window, it is capable to accommodate process changes by simply modifying some physical parameters of the model directly. In these experiments, since only the illumination source (S1) was swapped by a new SMO result (S2) with some dose adjustment, we expect to do the same operation directly on the existing model (M1) to simulate the new process quickly and conveniently.

If we do not have any metrology data for the new process, the best guess is that the anchor pattern would be printed on target at its best focus. Therefore, there are four steps to modify the existing model M1. First, replace the old illumination with the new source map, while keeping all other mask, optical and resist parameters unchanged. Second, adjust the dose to make the anchor pattern print on target. Third, simulate the Bossung curve of the anchor pattern to find the best focus value. Forth, adjust the dose again to make the anchor pattern on target at the best focus point. This results in the M2S model.

This process can also be regarded as a kind of “calibration” of the new defocus and anchor dose assuming perfect process tuning on anchor pattern and ideal model separability. However, using the anchor pattern only for “calibration” may have some “pattern coverage” concerns. The anchor pattern usually is not sensitive to defocus change, the real anchor CD may not be exactly on target and may not be mask error free. All those uncertainties may impact the full chip, full process window prediction power of the new model M2S. Some metrology data on the new process would be helpful to verify the accuracy of the regenerated model and “calibrate” dose and defocus with more realistic CD values. To enhance pattern coverage with well-controlled metrology cost, Tachyon FEM+ platform offers a FEM gauge selection tool, based on resist term response and optical sensitivity estimation. It is designed to maximize pattern representation capability of a subset of gauges to a full gauge set. The user just needs to specify the optical model of the swapped source and the number of gauges according to the metrology budget. The tool can then output a selected gauge set.

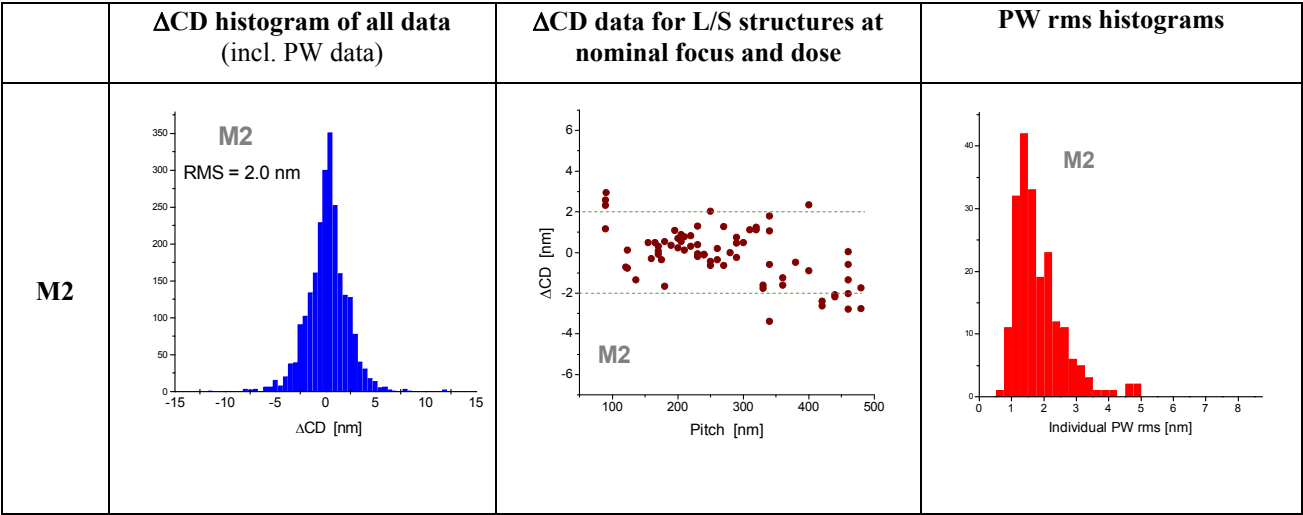
In this work only about 50 different gauges were used. With this limited metrology set from the new process, we can perform a “fitting” flow instead of simple anchoring. Besides fine tuning best focus with FEM data, we also adjust resist threshold while fixing all the other resist parameters. The threshold was adjusted to achieve the smallest RMS on the limited wafer measurements. With this real wafer data, the uncertainty of source swapping was further reduced. This procedure leads to the M2E model.

4. EVALUATION OF MODELS M2S AND M2E

4.1 Model error for calibration and verification gauges

The most obvious way of comparing the different models that were generated for source S2, is by using the kind of metrics that we normally use for model evaluation, as sketched in section 2. The three different models (M2, M2S and M2E) do however not share a common division of the experimental data into calibration and verification data (most of the data that served for calibrating M2 can only serve as verification data for models M2S and M2E). Therefore, we will do the model evaluation in this section on all the available CD data simultaneously. Figure 3 shows some of these comparison results.

The first observation is that – as expected - the completely independently calibrated model M2 is more accurate than the derived models (M2S and M2E): this appears from most of the metrics we applied to this comparison. We see that the RMS of the M2S model (3.3 nm) cannot reach the level of the M2 model (2.0 nm). But after performing the anchoring based on the limited experimental data (M2E) the RMS is lowered to 2.66 nm. Overall model M2E is performing better than M2S in that (for example) there seems to be no trend of $\Delta CD(Pitch)$ for the L/S structures. Also, the extreme values in the ΔCD data of M2S are somewhat larger than for M2E. This underlines the importance of anchoring a derived model based on some experimental data.



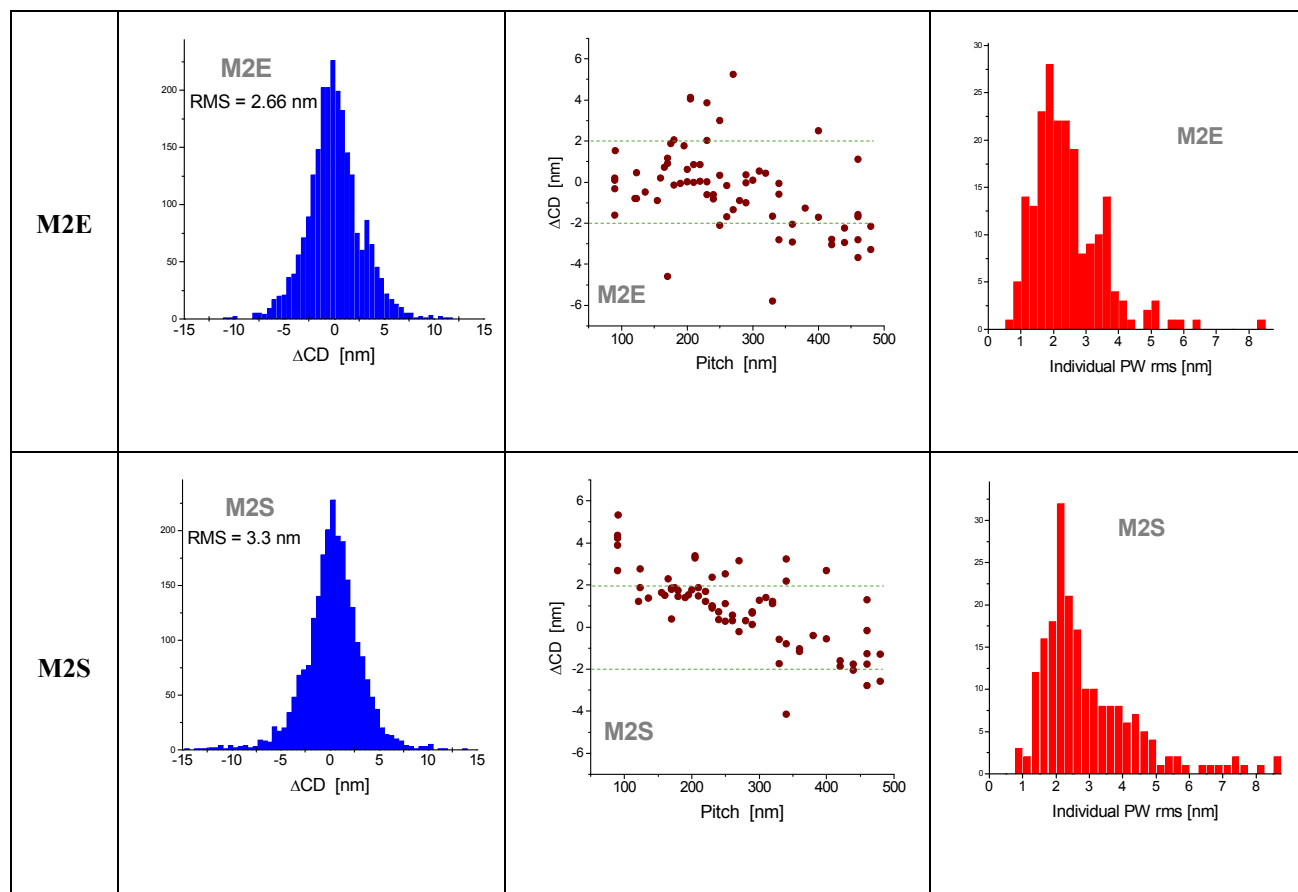


Figure 3: Application of some of the model-quality metrics of section 2, to compare models M2, M2S and M2E.

4.2 Deviation of contours from reference model

In the previous part we showed that the fully calibrated M2 model describes the experimental data well. This model gives us an upper limit as to what can be expected from a resist model for this source and process. In this section we would like to investigate how close the M2S and the M2E models are with respect to the M2 model in terms of printed contour prediction. To do this we will compare the contours of these two models with the contours of M2 on the 20nm node logic Metal1 layer of our test chip. The OPC for which we will compare the contours was performed with the M2 model.

In figure 4(a), we show the typical deviation of the contour calculated by the M2S model with respect to the contour calculated by the M2 model. In figure 4(b) and (c) we plot a histogram of the deviation of the M2S contour and M2E contour respectively with respect to the M2 model in nominal condition, calculated on a very large number of sampling points. We can see that the M2S model has an average error of 0.24 nm and a standard deviation of 0.39 nm, which indicates that the contours are quite close to the reference M2 model. When we take a look at the M2E model, we see that we can reduce the average error to -0.02 nm and further narrow down the distribution slightly to a sigma of 0.37 nm by using a limited set of gauges as described in the previous section.

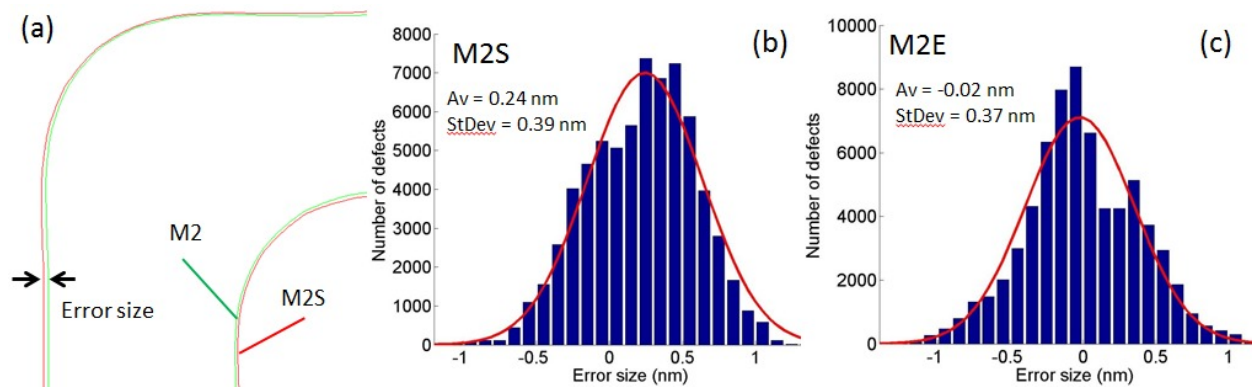


Figure 4: (a) Contour difference between M2S and M2. (b-c) Histogram of error size of model M2S and M2E respectively on a 20nm node metal 1 layer in nominal condition. The average of the Gaussian fit is 0.24 nm and the standard deviation is 0.39 nm for M2S while for the M2E model we obtain an average of -0.02 nm and a standard deviation is 0.37 nm.

We also investigate the average and standard deviation of the fitted Gaussian through focus and dose. Using Tachyon LMC (Lithography Manufacturing Check) we can compare the contour of the M2S and M2E models to the contour of the M2 model through dose and focus. In figure 5 we plot the average and standard deviation of the Gaussian fit to the histograms of M2S [figure 5(a)] and M2E [figure 5(b)] through focus and dose.

It is clear that the M2S model has a dependence on focus. The average is roughly linear with focus which indicates that the best focus of the M2S model is slightly offset with respect to the M2 model: in our case the M2S model is shifted to negative defocus leading to a positive offset at negative defocus and a negative offset at positive defocus. The standard deviation is much less dependent on focus and dose. The deviation from M2 stays below 2.3 nm (3σ), which indicates that even through focus and dose the model behaves quite accurately.

This deviation from M2 can clearly be reduced by determining the best focus and best dose for the model with our limited set of experimental data. In this case the average of the M2E model is much lower, indicating that the best focus is more precisely determined by using our small set of gauges. The standard deviation is roughly similar to M2S. In this case the total error across the PW stays below 1.7 nm (3σ).

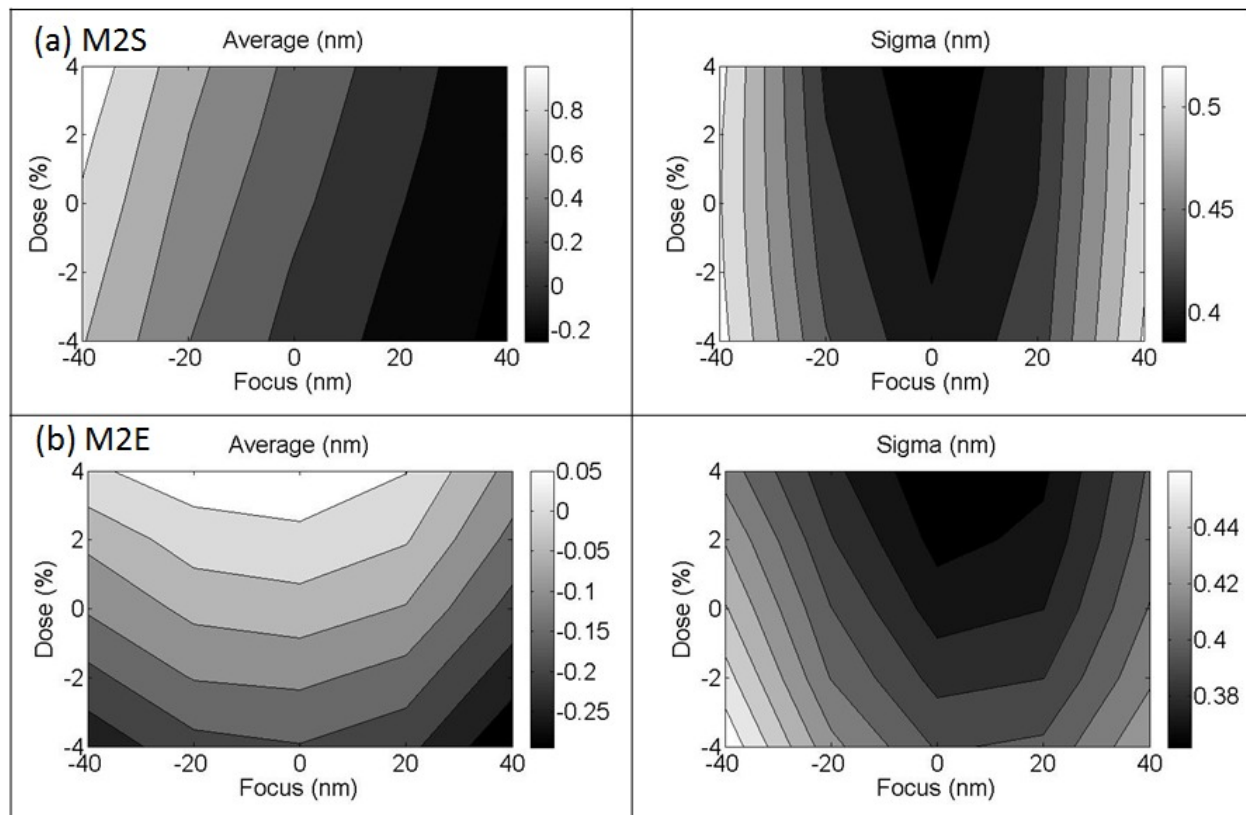


Figure 5: Average model error and standard deviation with respect to the M2 model through focus and dose for (a) the M2S model and (b) the M2E model.

4.3 Evaluate the impact of the derived models on OPC and PW

In this last part we want to quantify the effect of using the M2S and M2E model during OPC on the predicted PW of our Metall logic application. As was shown in the previous section, the M2S and M2E deviate slightly in the calculated contours from the optimal M2 model. These differences will lead to small changes in OPC-solution with respect to the reference OPC, run with the M2 model. The OPC-solution obtained with models M2S and M2E might be off, as these models themselves are not as accurate as model M2. The goal of this part is to quantify the loss in PW due to these inaccuracies in the OPC-solution induced by the error in the M2S and M2E models.

We evaluated this in the following way.

- First we run OPC on the same logic design with each of the three models M2, M2S and M2E separately.
- Second, we calculate the expected PW for each of these three cases, using Brion's LMC software. As we consider that model M2 is the more accurate of the three models, we use M2 for this PW calculation *for all three* OPC solutions. In this way, possible inaccuracies in the OPC result will show up as loss in the size of the process window we obtain. The detectors which are used in LMC and their corresponding thresholds are summarized in Table 2.

Table 2. Overview of the detectors and their thresholds used in LMC to determine the PW.

Detector	Target CD	Threshold
Necking_01	97 nm	80 nm
Necking_02	56-60 nm	48 nm
Bridging	65 nm	48 nm
Bridging LE	65 nm	48 nm
Line end push out/ pull back	/	+/-10nm

We start by comparing the PW without including any mask error in the calculation. In figure 6 it can be seen that the PW (fitted by an ellipse) for our reference OPC (M2) has a depth of focus (DoF) of 123 nm at 5% exposure latitude (EL) for our selected thresholds. In this case little difference is seen between M2S and M2E. More interestingly, both perform nearly as well as the reference model, indicating that our models are separable.

In figure 6(b) the effect on the OPC due to the small differences in contour calculation is depicted. Typically the main features have deviations of about 1-2 nm. Bigger differences concern assist features (AF). OPC model is used to perform AF printing check and adjust AF dimensions accordingly. Thus a different model may lead to different AF shrinkage.

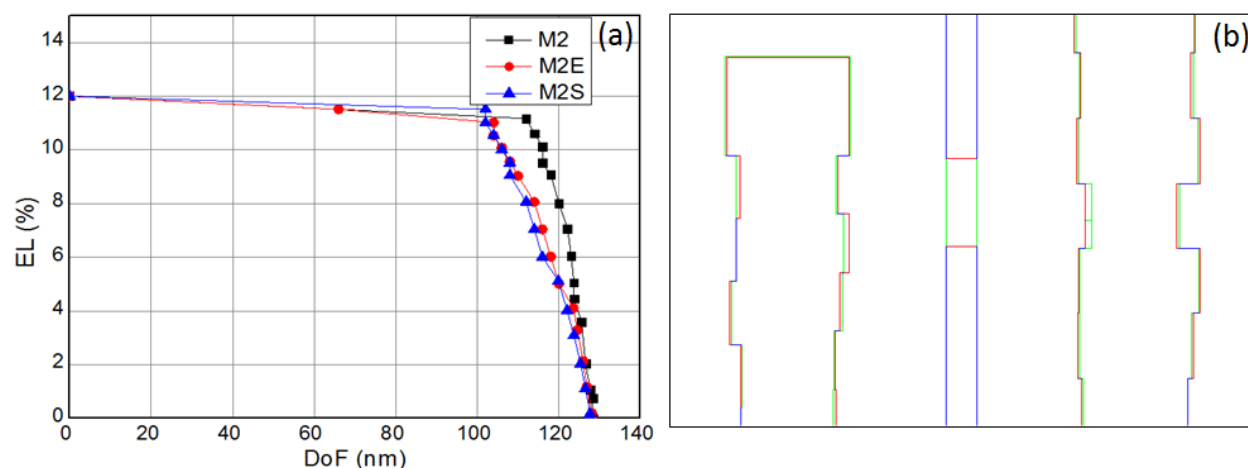


Figure 6: (a) PW of OPC run with M2, M2S and M2E model. PW is evaluated with M2 model for all three cases. (b) Section of design showing the OPC solution of model M2 and M2S.

Next, we re-evaluate the predicted PW if we do include a ± 0.5 nm mask error in the evaluation. Figure 7 shows the result for model M2. Three of the plots represent a dose-focus matrix, in which each of the dose-focus fields is given a color depending on whether or not a defect (i.e. a structure that violates the specs of Table 2) occurs. Green (or light grey) means that not a single defect occurs; red (or dark grey) means that at least one defect has been found. The green area in these plots therefore represents the process window. The left two pictures of Figure 7 show the result for a mask bias of $+0.5$ nm and -0.5 nm separately. The overlap is then defined as the total PW (see top right in figure 7). For the OPC obtained with our reference model M2 and again using the detectors listed in Table 2, we obtain a $\text{DoF}@5\%EL$ of 104 nm and an EL of 11.5% on our 20nm node Metal1 layer (see bottom right in figure 7).

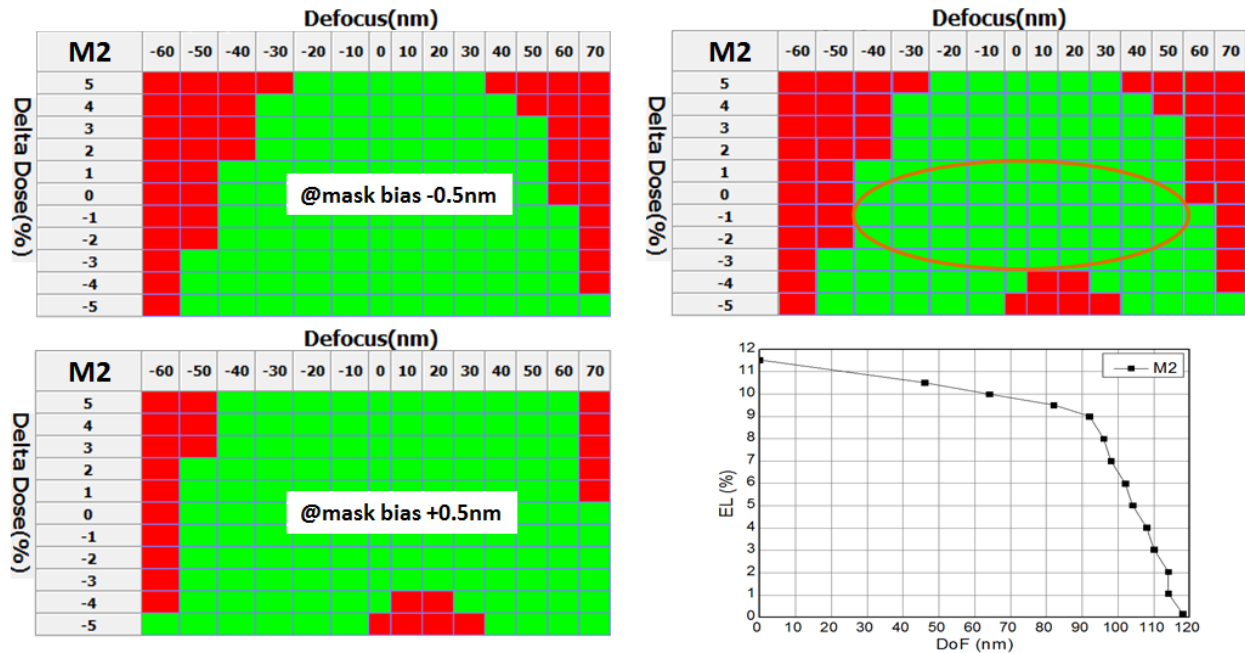


Figure 7: PW of OPC run with M2 model. The PW with a mask bias of ± 0.5 nm is depicted on the left, while the overall PW is shown on the top right. The corresponding exposure-defocus latitude plot is shown on the bottom right.

A similar analysis was done using the OPC result obtained with models M2S and M2E (still using M2 to calculate the PW, as explained). The result is shown in Figure 8. Here we see that the PW for the M2S model is decreased substantially: DoF@5%EL is 84 nm, while the EL is about 7.5%. In this case the benefit of M2E is clearly visible: the DoF@5%EL now is 92 nm, while the EL is about 11%. So in this case only about 10 nm is lost in DoF and about 1% in EL with respect to the reference OPC. We believe that the larger loss in PW of the M2S model when taking mask errors into account, indicates that performing the OPC with a model which is slightly in defocus leads to a higher MEEF.

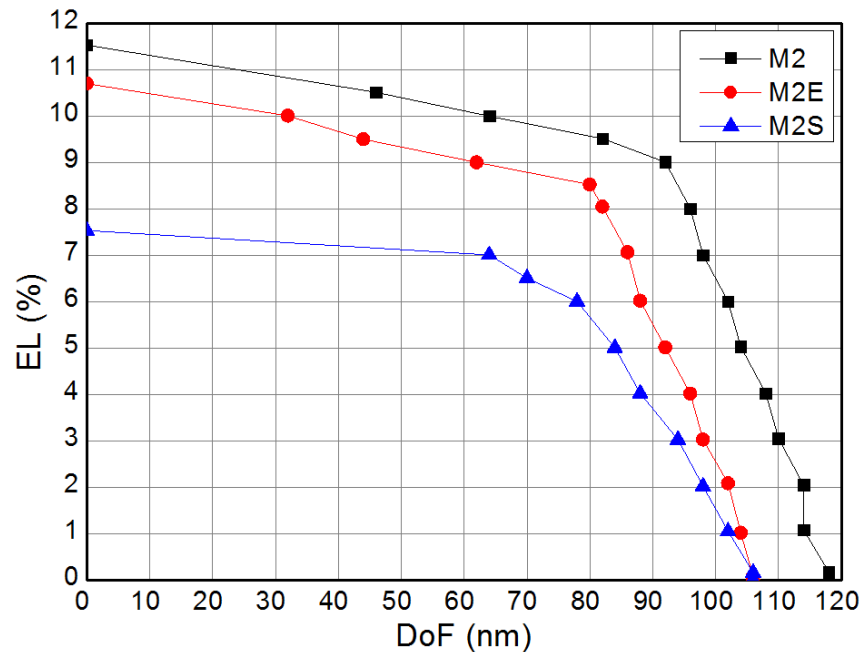


Figure 8: (a) PW for OPC solution obtained with models M2, M2S and M2E. The PW is calculated assuming a mask error up to ± 0.5 nm.

5. CONCLUSIONS

In this study, we compared OPC model prediction for a fully calibrated OPC model (M2) with models derived from a previously calibrated model obtained from a different illumination source, focus and exposure dose (M1). A full model calibration is quite labor (and tool time) intensive, which makes the possibility of using such derived models (for which only a limited set of new wafer measurements is needed) an attractive possibility. Of course, some loss in prediction accuracy can be expected (if the optical and resist model parts are not completely separable), and this paper quantified the possible trade-off one may face in the resulting printing performance on wafer.

We compared the three models of this study (M2, M2S and M2E) by looking at direct model-quality metrics and differences in predicted contours but perhaps the most telling comparison is the one of section 4.3, in which we looked at predicted process window. This shows that the fully calibrated model (M2) offers the largest simulated process window, as could be expected, and that using model M2S would lead to a loss in PW due to inaccurate best focus determination based on simulated anchor Bossung curve. Determination of best focus and dose is important for model predictability power and simply relying on anchor pattern simulation would lead to higher degree of uncertainty compared to limited set of experimental data. Including mask errors to determine the PW, for model M2S we lose about 20 nm DoF and 4% EL with respect to model M2. After determining the BF and BD more accurately with wafer data, the predicted performance of model M2E lies somewhere in between: now we lose roughly 10 nm in DoF and 1% in EL with respect to the optimal model.

This shows that it is possible to derive a new model from an existing one that has good separability while using only a limited amount of additional wafer data. In this way a trade-off can be made between the effort and tool-time required for additional wafer measurements, and the PW performance obtained.

REFERENCES

- [1] Liu, H.-Y., Zhao, Q., Chen, J. F., Jiang, J., et al., "*Separable OPC models for computational lithography*" Proc. SPIE 7028, 70280X (2008)
- [2] Hunsche, S., Xie, X., Zhao, Q., et al., "*Scanner-specific separable models for computational lithography*" Proc. SPIE 7122, 71221V (2009)
- [3] Van Look, L., Bekaert, J., Truffert, V., et al., "*Printing the metal and contact layers for the 32- and 22-nm node: comparing positive and negative tone development process*" Proc SPIE 7640, 764011 (2010)
- [4] Liu, P., Zuniga, C., Ma, Z., Feng, H., "*Validation of a fast and accurate 3D mask model for SRAF printability analysis at 32nm node*" Proc SPIE 6730, 67301R, (2007)